MAGNETOHYDRODYNAMICS Vol. 51 (2015), No. 2, pp. 257–265

A REPORT ON THE FIRST NEUTRON RADIOGRAPHY EXPERIMENT FOR DYNAMIC VISUALIZATION OF SOLID PARTICLES IN AN INTENSE LIQUID METAL FLOW

M. Ščepanskis[1], *M. Sarma*[2], *R. Nikoluškins*[2], *K. Thomsen*[3], *A. Jakovičs*[1], *P. Vontobel*[3], *T. Beinerts*[2], *A. Bojarevičs*[2], *E. Platacis*[2]

[1] *Laboratory for Mathematical Modelling of Environmental and Technological Processes, University of Latvia, 8 Zeļļu str., LV-1002, Rīga, Latvia*
[2] *Institute of Physics, University of Latvia, 32 Miera str., LV-2169, Salaspils, Latvia*
[3] *Paul Scherrer Institute, Villigen PSI, CH-5232, Switzerland*

The present paper contains a report on the first neutron radiography experiment that visualized the motion of solid particles in liquid gallium in a rectangular vessel, which was stirred by a system of four counter-rotating magnets. The experiment has demonstrated that the neutron radiography is a promising experimental method for the investigation of dynamics of particles in liquid metal.

Introduction. This paper deals with electromagnetically (EM) induced recirculated flows of liquid metal that are typical for metallurgical applications, e.g., induction furnaces and stirrers. Such flows were studied numerically and experimentally since the 1970's and achieved significant progress in the XXI century with the rapid increase of computational resources, which now allow to run Large Eddy Simulation (LES) models for industrial applications, and the development of more precise measurement techniques (see, e.g., [1, 2]). Now, the dynamics of solid inclusions in these flows, i.e. the two-phase case, has posed a new challenge. General industrial interest for this problem is connected with the optimization of admixing and homogenization of alloying inclusions and refractory erosion in the metallurgical industry.

Homogenization of solid inclusions in an induction crucible furnace (ICF) was simulated, using the LES method, by Ščepanskis *et al.* [3] and a model for industrial use was proposed [4]. Despite the relative success in the Lagrangian modelling of such particle laden flow, an experimental investigation of particles in turbulent flow of liquid metal poses an extremely complicated challenge, and the first attempt to measure the particle concentration field in a small ICF was done only last year [5]. Nevertheless, the mentioned experiment was able to measure the concentration field only at the dynamically equilibrium stage. The present paper reports about a new experimental technology in this context: neutron radiography that is able to fill the gap of the experimental investigation of particles in liquid metal. Moreover, the authors believe that in prospect dynamic neutron radiography of small particles in low-melting-temperature alloys can be used for non-invasive investigation of liquid metal flows similar to the particle image velocimetry (PIV) technique.

In fact, the first known neutron radiography of a two-phase liquid metal flow was performed by Saito *et al.* in 2004 [6]. Rising gas bubbles were visualized in the Pb-Bi eutectic and the PIV technique was already applied to investigate the flow. However, the flow was initiated only by the rising bubbles without any EM stirring; therefore, the intensity of the flow was low and the bubbles were

big. Thus, the present experiment can be considered as a significant step forward, while the visualization of particles in an intense EM induced flow is performed.

When choosing a particular setup for the experiment, we have concluded that most of the industrial applications are associated with cylindrical geometries of a vessel filled with a liquid metal that is stirred by a solenoidal inductor. A widespread example of such technology is the already mentioned ICF [7]. The aternating current in the inductor around the crucible induces a current in the melt and a magnetic field, which results in a Lorentz force that moves the liquid metal and forms counter-rotating vortices. However, such device is not convenient for the neutron radiography investigation for some reasons: 1) the water-cooled inductor will be in the way of the neutron beam; 2) in order to stir up a small volume of liquid metal, which is limited by the absorption of neutrons by the matter, a high frequency generator which is big and massive, should be transported to the neutron source.

At the same time, permanent magnet systems are suitable for experiments and can produce the same flow pattern, as it was described above, but they are very rare in industrial metallurgical applications due to the temperature limitation imposed by the magnets; however, recent and still unpublished Bojarevičs′ and Beinerts′ inventions also found an industrial use of such technology for the stirring of aluminum. Moreover, lately other authors also began to report investigations of permanent magnet systems (see, e.g., [8]) and outlooks on their industrial usage. In addition, an application of rotating cylindrical magnets for pumping aluminum was reported [9, 10] and liquid metal pumps with magnets integrated in a single rotating cylinder or double disk are also well-known (see, e.g., [11]). These applications strengthen our motivation to use a permanent magnet stirrer for the neutron radiography experiment. In this case, a rectangular geometry of the vessel, which is more convenient for neutron radiography, is possible.

1. Neutron radiography method. We expect that a reader of the *Magnetohydrodynamics* journal is not much familiar with neutron radiography. Therefore, here we provide a short description and explanation of the basic phenomena taking place at neutron radiography.

The main advantage of neutron radiography in contrast to X-ray radiography, which brings the first one forward in an attempt to look through a liquid metal layer, is associated with different attenuation properties of the corresponding beams. X-rays attenuate relative to the material's density; it is an electromagnetic radiation which mainly interacts with the electrons of an atom. Hence, the more electrons an atom has (i.e. with the increasing atomic number), the higher the probability for X-ray interaction. Therefore, less than a centimeter thin layer of heavy metal significantly eliminates an X-ray beam of usual energy. This fact makes impossible classical radiography of low temperature alloys which usually contain heavy metals like lead, bismuth, gallium, etc., in a vessel of a thickness that is enough for the development of turbulent flow. In the known investigations in iron [12] and aluminum [13, 14], the crucible used has to be of the order of the bubble diameter to permit X-ray penetration through the metal [13]. Therefore, X-rays are not suitable for the analysis of small inclusions in the intense flow of liquid metal.

Contrary to X-rays, neutrons interact on the level of the nucleus. Therefore, the neutron is quite sensitive to light atoms like hydrogen, oxygen, etc. which have much higher interaction probability with neutrons than with X-rays. In contrast to this, metals show a comparatively lower interaction probability with neutrons, thus allowing quite a high penetration depth. Table 1 compares the

Table 1. Attenuation coefficients of thermal neutrons (α_N) and 150 kV X-ray (α_X) for the selected materials. For more materials see the source table in [15].

element	atomic number	α_N, [cm^{-1}]	α_X, [cm^{-1}]
hydrogen (H)	1	3.44	0.02
boron (B)	5	101.60	0.28
carbon (C)	6	0.56	0.27
oxygen (O)	8	0.17	0.16
sodium (Na)	11	0.09	0.13
magnesium (Mg)	12	0.15	0.24
aluminium (Al)	13	0.10	0.38
silicon (Si)	14	0.11	0.33
calcium (Ca)	20	0.08	0.26
iron (Fe)	26	1.19	1.57
gallium (Ga)	31	0.49	1.42
cadmium (Cd)	48	115.11	4.84
indium (In)	49	7.58	4.31
tin (Sn)	50	0.21	3.98
gadolinium (Gd)	64	1 479.04	8.69
lead (Pb)	82	0.38	22.81
bismuth (Bi)	83	0.27	20.28

attenuation coefficients for neutrons (α_N) and for X-rays (α_X) in the selected materials. Transmission of the initial beam can be calculated according to the universal Beer–Lambert law:

$$I = I_0 e^{-\alpha_{N,X} d}, \tag{1}$$

where d is the thickness of a sample in the beam direction; I and I_0 denote the intensity of the beam after and before passing the sample.

The experiment, which is reported in the present paper, was done at the Swiss Spallation Neutron Source (SINQ) in Paul Scherrer Institute (Villigen, Switzerland). SINQ is presently a world's highest flux accelerator-based continuous neutron spallation source. It is situated at the end of a cascade of three accelerators that deliver a proton beam of 590 MeV at a current up to 2.3 mA. The spallation target is an array of lead rods that produce a continuous neutron flux of about 10^{14} n/cm^2/s. Instruments extract neutrons by evacuated flight tubes and neutron guides from the D_2O moderator tank or a liquid D_2 cold source.

The thermal neutron transmission radiography facility (NEUTRA) consists of evacuated neutron flight-tubes looking through a 20 mm diameter pinhole into the heavy water SINQ moderator tank. It allows neutron radiography and tomography images of objects of medium to large size using a thermal neutron energy spectrum. The neutron energy in this facility is about 25 meV; the neutron flux depends on the proton current delivered to SINQ and is not more than 5×10^6 neutrons cm^{-2}sec^{-1}mA^{-1} (p-current) at the sample position.

The primary detection reactions for thermal neutrons are mainly neutron capture by an absorbing material emitting charged particles. The scintillator screen (200 μm thick Li^6 doped ZnS) produces light when excited by ionizing radiation. This light is reflected perpendicularly to the neutron beam direction while neutrons pass through the mirror as shown in Fig. 1. The reflected light is recorded by a CCD or a CMOS camera. An Andor Neo sCMOS pixel detector is used in the NEUTRA. We refer to [16] for more detailed information about the detectors and the proper reactions.

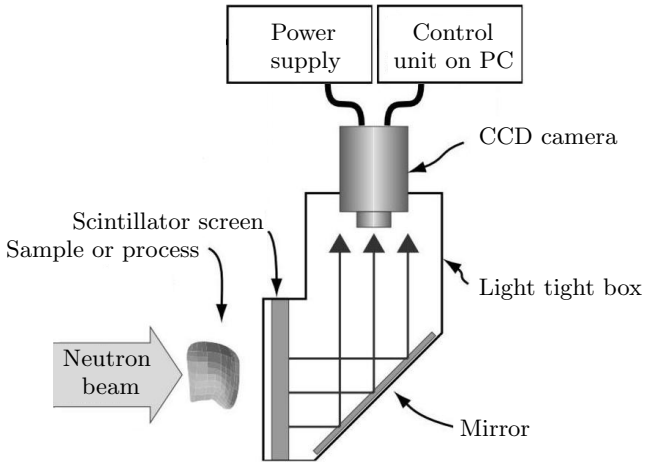

Fig. 1. The design of devistandard combination of a CCD camera and a neutron scintillator for neutron imaging [16].

Generally, for more information about the NEUTRA facility, we refer the reader to [17] as well as to the webpage of Paul Scherrer Institute.

2. Experiment. Because the classical induction system was not convenient for the neutron radiography experiment (two-dimensional), a design, which contained counter-rotating cylindrical magnets, was chosen. Such a design allows sparing a high frequency generator and an inductor; however, an additional mechanical system, including gears, belts and bearings, had to be created to ensure rotation of the magnets. The stirrer consists of three main units: 1) the block of shafts with rotating magnets on one side and belt pulleys on the other side; 2) the frame with a motor and driving elements, gears and pulleys; 3) the rectangular vessel with glass walls on the front and on the back sides, the small heating element on the bottom. The mentioned units are marked in the sketch of the setup (Fig. 2*a*). The rectangular vessel for liquid metal (marker 3 in Fig. 2*a*) is made of window glass which contains silica (SiO_2) 72%, sodium oxide (Na_2O) 14.2%, lime (CaO) 10.0%, magnesia (MgO) 2.5%, alumina (Al_2O_3) 0.6%; all these materials have low attenuation coefficients. The stirrer is constructed in such a way that nothing is situated on the line of the neutron beam, it only has to pass twice the 2 mm glass.

The inner size of the vessel is $100\times100\times30$ mm. Apparently, the width of the vessel is limited by the width of the neutron beam, and the size along the direction of the beam is optimized with respect to the beam attenuation by the liquid metal. Thus, according to expression (1), the 3 cm gallium will leave 23% of the initial intensity of the beam.

The magnets are 30 mm in diameter and 50 mm long; the distance between the centers of the closest magnets is 50 mm; the distance from the edge of the magnets and liquid metal is 9 mm. The vessel is centered with respect to the magnets in the direction of the neutron beam.

The experimental setup was designed to excite two different schemes of rotation (see Fig. 3). Such a design made it possible to examine several different flow configurations within the same vessel.

In order to choose a proper metal for the experiment, two properties should be considered: 1) the low melting temperature to avoid heating close to a de-

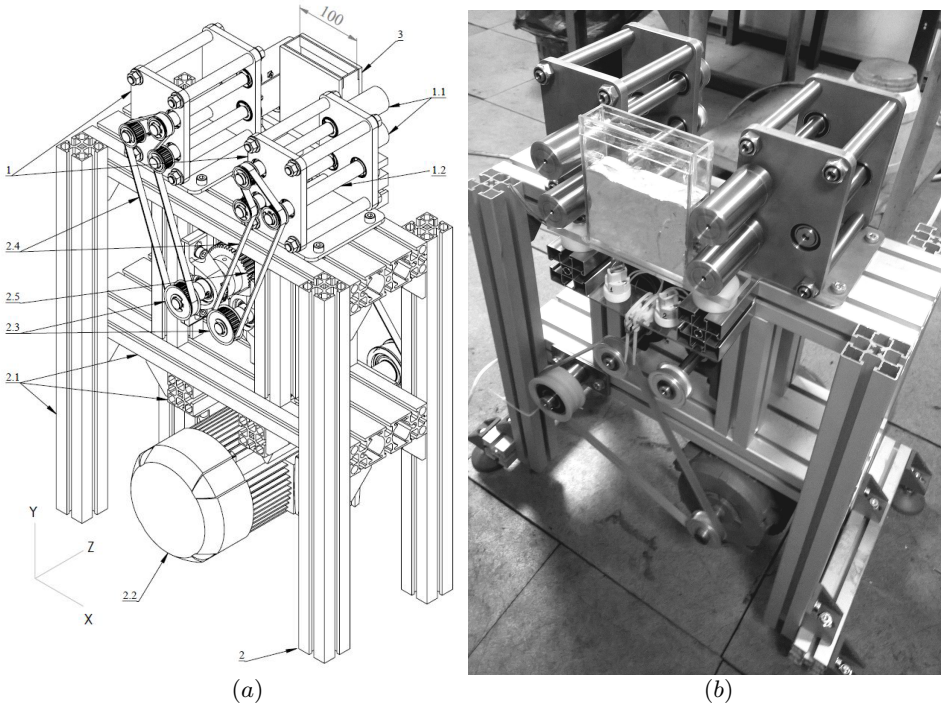

(*a*) (*b*)

Fig. 2. The experimental set up: (*a*) a sketch; (*b*) a photo.

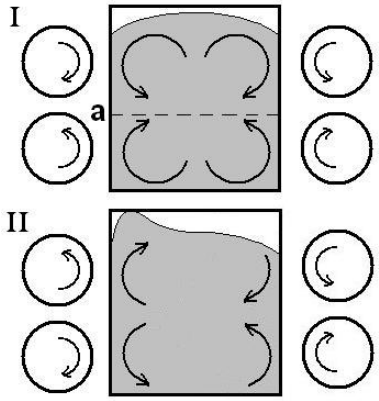

Fig. 3. The schemes of two possible rotation directions of the permanent magnets.

tector and camera that should be situated as close to the vessel as possible; 2) the attenuation of the neutron (see Table 1). It becomes clear that low temperature eutectics, which contains cadmium (Cd) and indium (In), such as Wood's metal and Galinstan, cannot be used because of high values of the attenuation coefficients. Bismuth (Bi) is also unwanted because it can be activated in the neutron beam and tiny amounts of polonium (Po) can appear. For these reasons, we chose gallium (Ga), which is acceptable for neutron radiography and has a suitable melting temperature (30 °C).

The material properties of the inclusions used for the neutron radiography experiment have to fulfill various requirements. The attenuation coefficient of the particles cannot be in the same range as that of the liquid metal, otherwise

they will be invisible. Therefore, the typical SiO_2, ZrO_2 and Al_2O_3 oxides are useless here. Boron carbide (B_4C), which has a very high attenuation coefficient (see Table 1), was found to be good for the experiment. However, due to its low density ($2.52\,g/cm^3$) and the very low size of available particles, it was a significant problem to mix such powder from the surface into the metal. Therefore, special particles, which consisted of a lead (Pb) kernel, which is a heavy material, and boron carbide powder glued around the kernel, were produced. The diameter of the particles was 3.8 ± 0.5 mm, and the average density was a little bit less than that of gallium ($6.1\,g/cm^3$) so that they were remaining on the top surface without stirring.

3. Results and discussion. As for the results of this experiment, we are happy to report the first images of dynamic visualization of the particles inside the stirred liquid metal, which became available by using the neutron radiography method. The short video-report of the present results is placed in the Appendix to this paper available on the webpage of the MHD journal [19].

Fig. 4 shows traces of particles at a high rotation speed of the magnets, 35 rps, in the configuration of the EM system, which produces a flow similar to that in the ICF. The rotation directions are shown in Fig. 3, case I. These images could be further postprocessed in order to make a firm conclusion about the flow pattern; nevertheless, a three-vortex structure may be recognized in some of the frames. Such structure was predicted numerically [18]. However, the flow is highly turbulent and other flow patterns like four counter-rotating vortices also appear.

Fig. 5 demonstrates that it is also possible to resolve the used particles as single points, but not the traces along the trajectories like in the previous figure. However, the level of noise increases with the decrease of exposure duration.

Fig. 6 shows images that correspond to a different rotation constellation of the magnets. The EM system here corresponds to case II (see Fig. 3). The very high hill of the melt free surface next to the magnet, which moves the liquid upward, is typical for this rotation scheme. The eddy, which forms this hill, is small in size, but the speed of liquid is high there; therefore, such a protuberance is stable.

The high level of the free surface in this case, even at a comparatively low rotation speed (12.6 rps), prevents the possibility to increase the stirring rate by speeding up the rotation. Nevertheless, it seems to be clear that such a stirring scheme is not effective if compared to the previous one; only few particles escape the surface and appear inside the melt.

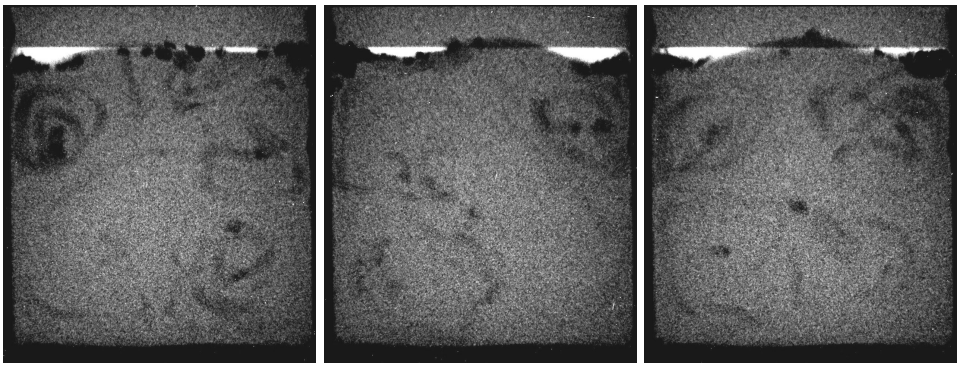

(*a*) (*b*) (*c*)

Fig. 4. Raw neutron images of particle motion in the liquid metal. Rotation scheme I (see Fig. 3); rotation speed 35 rps; exposure time 0.1 s.

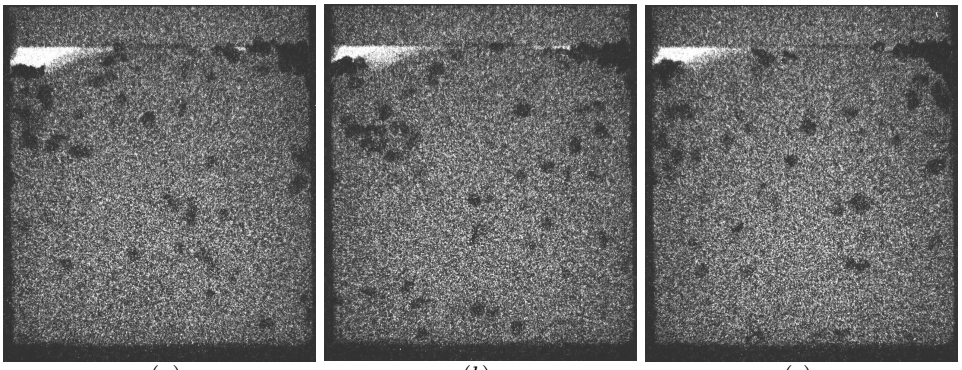

(*a*) (*b*) (*c*)

Fig. 5. Raw neutron images of particle motion in the liquid metal. Rotation scheme I (see Fig. 3); rotation speed 35 rps; exposure time 0.01 s.

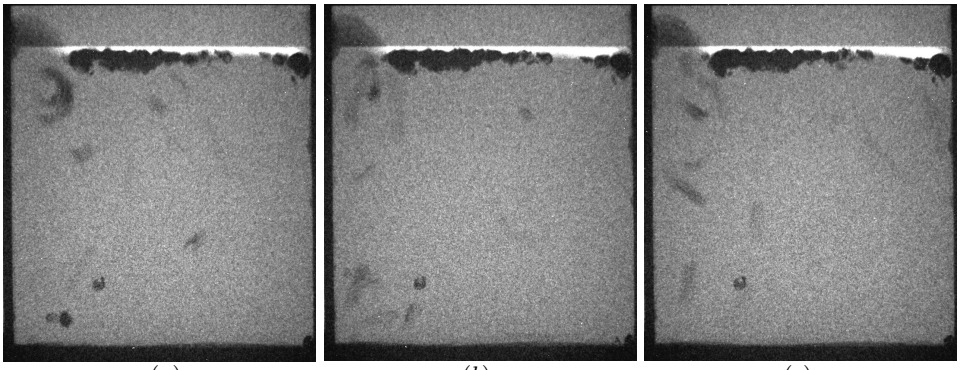

(*a*) (*b*) (*c*)

Fig. 6. Raw neutron images of particle motion in the liquid metal. Rotation scheme II (see Fig. 3); rotation speed 12.6 rps; exposure time 0.1 s.

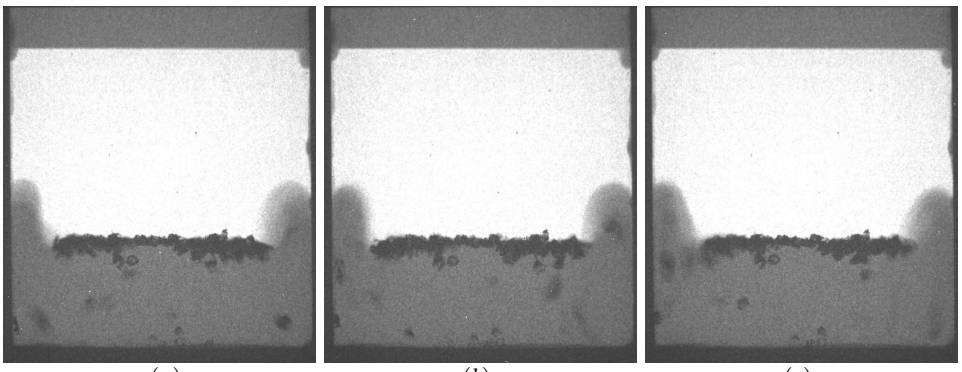

(*a*) (*b*) (*c*)

Fig. 7. Raw neutron images of particle motion in the liquid metal. Rotation scheme II (see Fig. 3); rotation speed 28.2 rps; exposure time 0.1 s..

Finally, the level of the liquid metal in the rectangular vessel was decreased so that the surface was adjacent to the upper edge of the lower magnets (case Ia in Fig. 3). Fig. 7 demonstrates for this case the very intensive protuberances of the metal next to the magnets. Few particles were entrained in the very fast spinning in these vortices, but the rest of the particles remained on the stable surface between the hills.

It should be mentioned that, generally, postprocessing of these raw images is a non-trivial task because of a couple of technical difficulties: 1) a high level of noise; 2) non-homogeneity of the beam intensity (without normalization, the central region is lighter than the periphery). Additionally, speed limits of the available detector system (the real frame rate of the images was about 1 fps) were a significant obstacle to obtain quantitative results, as the particle image velocimetry method does in transparent liquids. However, we believe that these technical problems can be solved in another experiment that is planned to be carried out in 2015. A high speed camera (up to 32 fps) will be available at the NEUTRA soon. The present team of researchers is going to produce better particles (smaller and more uniform) for the second experiment as well. Titanium boride and gadolinium oxide are the candidate materials for this goal.

4. Conclusions. The first results attempting the dynamic visualization of solid inclusions in the EM induced flows of liquid metal are reported in this paper. We were able to prove that neutron radiography is a suitable method for achieving the mentioned goal; however, some technical improvements of the experiment should be done in order to obtain more quantitative results that can better verify numerical models for the metallurgical industry.

The authors are going to perform careful postprocessing of the present experimental results as well as continue with numerical simulations of the actually used systems in order to compare the results in more details.

Finally, the authors would like to reveal the prospect of this experimental research for the development of a neutron particle image velocimetry method, which can be very useful for the metallurgical industry.

Acknowledgements. The research, which is the contribution of Dr. M. Ščepanskis, M. Sarma, R. Nikoluškins, Dr. A. Bojarevičs and Dr. E. Platacis, as well as the building and transportation of the setup were financially supported by the European Social Fund (project. No. 2013/0018/1DP/1.1.1.2.0/13/APIA/VIAA/061).

The experiment was performed at the Swiss Spallation Neutron Source SINQ, Paul Scherrer Institute, Villigen, Switzerland, which also supported the PSI-authors.

The authors are also grateful to V. Geža and Prof. B. Nacke (Institute of Electrotechnology, Leibniz University of Hanover) for the preparation of solid samples for a preliminary neutron tomography experiment. The results of the experiment were not directly used in the present investigation; however, it was necessary to get a permission to carry out the experiment, which is reported in this paper, at SINQ.

REFERENCES

[1] A. Bojarevics, V. Bojarevics, Yu. Gelfgats and K. Pericleous. Liquid metal turbulent flow dynamics in a cylindrical container with free surface: experiment and numerical analysis. *Magnetohydrodynamics*, vol. 35 (1999), no. 3, pp. 205–222.

[2] A. Umbrashko, E. Baake, B. Nacke and A. Jakovics. Modelling of the turbulent flow in induction furnaces. *Met. Mater. Trans. B*, vol. 37B (2006), pp. 831–838.

[3] M. Ščepanskis, A. Jakovičs and B. Nacke. Homogenization of non-conductive particles in EM induced metal flow in a cylindrical vessel. *Magnetohydrodynamics*, vol. 46 (2010), pp. 413–423.

[4] M. Ščepanskis, A. Jakovičs, E. Baake and B. Nacke. A model for homogenization of solid alloying admixtures in an induction crucible furnace. *Steel Research Int.*, vol. 86 (2015) pp. 169–174.

[5] M. Ščepanskis, A. Jakovičs, E. Baake and B. Nacke. Solid inclusions in an electromagnetically induced recirculated turbulent flow: Simulation and experiment. *Int. J. Multiphase Flow*, vol. 64 (2014), pp. 19–27.

[6] Y. Saito, K. Mishima, Y. Tobita, T. Suzuki and M. Matsubayashi. Velocity field measurement in gas-liquid metal two-phase flow with use of PIV and neutron radiography techniques. *Appl. Radiation and Isotopes*, vol. 61 (2004), pp. 683–691.

[7] F. Hegewaldt, H. Gillhause and O. Erdman. *Induction Crucible Furnace*. Patent US 3944715 A, 16.03.1976.

[8] B. Mikhailovich, O. Ben-David, A. Levy. Liquid metal rotating flow under permanent magnetic system impact.. *Magnetohydrodynamics*, vol. 51 (2015), no. 1, pp. 171–176.

[9] T. Beinerts, A. Bojarevics, Yu. Gelfgat and I. Bucenieks. Linear permanent-magnet pump and stirrer for molten aluminum. *J. Iron Steel Res. Int.*, vol. 19 (2012), suppl. 1, pp. 528–530.

[10] A. Bojarevičs, J. Gelfgats, T. Beinerts, I. Bucenieks. *Metāla sakausējuma sūknēšanas un maisīšanas peņēmiens un iekārta tā realizēšanai*. Patent LV 14404 B, 20.10.2011 (in Latvian).

[11] I. Bucenieks and K. Kravalis. Efficiency of EM induction pumps with permanent magnets. *Magnetohydrodynamics*, vol. 47 (2011), no. 1, pp. 89–96.

[12] M. Iguchi, T. Chihara, N. Takanashi, Y. Ogawa, N. Tokumitsu and Z. Morita. X-ray fluoroscopic observation of bubble characteristics in a molten iron bath. *ISIJ Int.*, vol. 35 (1995), no. 11, pp. 1354–1361.

[13] V.F. Chevrier and A.W. Cramb. X-ray fluoroscopy observations of bubble formation and separation at a metal-slag interface. *Met. Mater. Trans. B*, vol. 31B (2000), pp. 537–540.

[14] X. Dai, X. Yang, J. Campbell and J. Wood. Effects of runner system design on the mechanical strength of Al-7Si-Mg alloy castings. *Mater. Sci. Eng. A*, vol. 354 (2003), pp. 315–325.

[15] http://www.psi.ch/niag/comparison-to-x-ray.

[16] http://www.psi.ch/niag/neutron-imaging-detectors.

[17] E.H. Lehmann, P. Vontobel and L. Wiezel. Properties of the radiography facility NEUTRA at SINQ and its potential for use as European reference facility. *Nondestr. Test. Eval.*, vol. 16 (2001), pp. 191–202.

[18] M. Ščepanskis, R. Nikoluškins, A. Bojarevičs, T. Beinerts, V. Geža, A. Jakovičs and K. Thomsen. Liquid metal flow induced by counter-rotating permanent magnets in rectangular crucible. In: *Proc. the 9th International* Pamir *Conference on Fundamental and Applied MHD, Thermo Acoustic and Space Technologies*, Riga, Latvia, 2014, vol. 1, pp. 278–282.

[19] http://mhd.sal.lv/contents/2015/2/ScepanskisEtAlNeutronRadiography.wmv.

Received 07.01.2015